Egyptian Journal of Chemistry
http://ejchem.journals.ekb.eg/

Removal of Reactive Yellow 160 from Aqueous Solution by Alumina Nanoparticles Derived from Aluminium Waste Residue

Hany H. Abdel Ghafar[1,2], Emad K. Radwan[2]*, Nagy M. Khalil[1,3], Yousif Algamal[1]

[1]*Department of Chemistry, College of Sciences and Arts at Khulais, University of Jeddah, Saudi Arabia*

[2]*Water Pollution Research Department, National Research Centre, 33 El Bohouth St, Dokki, Giza, Egypt 12622*

[3]*Refractories Department, Ceramics and Building Materials, National Research Centre, 33 El Bohouth St, Dokki, Giza, Egypt 12622*

IN the current study, alumina nano particles were prepared from waste aluminum residue by an extraction and gel formation method. The prepared alumina nanoparticles were used to remove reactive yellow 160 (RY160) from an aqueous solution. The kinetics and adsorption equilibrium were discussed as well.

The results show that, the heat-treated samples were consisting of Al and O elements only and their crystalline phase was pure alumina in the nano scale. The alumina nanoparticles were effective adsorbents for the removal of RY160 from aqueous solution with percentage removal 100 % for samples heat-treated at 110°C and 600°C. The adsorption data was well fitted to Langmuir isotherm model for all prepared samples indicating a monolayer adsorption. The adsorption process was found to be endothermic and the adsorption takes place physically on the surface of alumina nanoparticles. The prepared alumina nanoparticles samples can be used as an efficient adsorbent in water treatment.

Keywords: Adsorption, Wastewater treatment, Low-cost materials, Solid waste management, Kinetics and isotherms.

Introduction

The diminishing of freshwater resources due to mismanagement of water resources, population growth, and water pollution became an urgent problem threaten the world. One of the major concerns in water pollution, particularly in developing countries, is colored wastewater [1]. These include the waste streams from industries such as textile, paint and pigment, leather, plastics, rubber, cosmetics, pharmaceutical and food industries [1, 2]. Dye pollution increased due to the increasing of bulk global production of dyes. Meanwhile, the dye pollution can cause various human health effects and ecological deterioration due to their toxicity, mutagenicity, carcinogenicity and interference in the photosynthesis process of aquatic plants [3, 4]. Reactive azo dyes are the most widely used dyes in the textile industry, however, they are classified as environment unfriendly substances due to their toxicity and low biodegradability [4, 5]. Therefore, the removal of reactive azo dyes from water environment is an essential for saving environment and human health.

Several methods were proposed to remove dyes from wastewater including ion exchange, chemical precipitation, solvent extraction, anaerobic/aerobic biological degradation, coagulation, flocculation, precipitation, membrane filtration and advanced oxidation processes. However, these methods were found to be ineffective as they found to produce secondary waste [1,2,4,6].

A better alternative is adsorption, which has shown a high potential for the removal and

recovery of dyes from wastewater. It is ruled by simple operational and regeneration of the adsorbent. Moreover, adsorption gains a good reputation as a method of water treatment due to its numerous characteristics such as cost effectiveness, large scale application, simplicity, insensitivity to toxic materials, flexibility, availability of various adsorbents and high efficiency as practical and economic technique for dyes removal [1,2,5,6]. However, finding an efficient and low-cost adsorbent is critical for the adsorption process. Large number of low-cost materials was used as adsorbent including natural materials [7-9], algae [10], humic acids [9,11], clay minerals [8] viscose fiber, magnetic particles and wool fiber waste [12-15].

The growing interest of using nano-sized metal oxide as adsorbent in dye adsorption is attributed to its simple synthesis process, cheapness, high surface area and nontoxicity [13,16-19]. However, few studies have emphasized the advantages of aluminum oxide (alumina) nanoparticles for reactive dye adsorption.

The current study focused on the preparation of alumina nanoparticles from waste aluminum metal collected from workshops of aluminum kitchen, doors and windows as low-cost and environmentally friendly material. The prepared samples were characterized by different techniques and their efficiency for removing reactive yellow 160 (RY160) azo dye from aqueous solution was studied in details. The adsorption data was analyzed by the isotherm models.

Materials and Methods

Materials

Waste aluminum scraps were collected from workshops of alumina's kitchens, doors and windows workshops. Hydrochloric acid and ammonia solution were used during the extraction and precipitation of Al_2O_3.

Experimental

A representative sample of the aluminum waste was dissolved in 1:1 dilute hydrochloric acid. The filtrate was used to precipitate aluminum hydroxide through stepwise addition of 1:1 diluted ammonia solution. At pH 7 a white gel precipitate is formed. After settling for 24 hrs., the precipitate was dried for another 24 hrs. at 110°C then subjected to different heat treatment temperatures 110, 600, 800 and 1050°C for 1 h at heating rate 10°C /min. The prepared samples were referred to as Alo-110, Alo-600, Alo-800 and Alo-1050 according to the heat treatment temperature.

The prepared alumina nanoparticles were characterized using X-ray diffractometer (XRD), D8 ADVANCE, Bruker, Germany, (diffractometer with Ni-filtered Cu Kα radiation operating at 40 mA and 40 kV). The crystal size was calculated from the broadening of the XRD peaks using Scherer's equation: $D = k\lambda / \beta \cos \theta$, where β is the full width at half maxima of the XRD peak in radiant, θ is the reflection angle of the peak, k is a constant nearly equal 0.90 and λ is the wavelength of the diffracted X-rays.

The microstructure and spot analysis of some selected samples were tested using SEM (SEM; JEM-6460LV, Japan) attached with energy dispersive x-ray unit (EDAX).

The FTIR analysis of the prepared samples were performed using Jasco FT/IR-6100A instrument-Japan. All spectra were measured in the wavenumber range 4000–400 cm^{-1}. The surface area and pore volume analysis were performed using nitrogen adsorption at 77 K by a BELsorp max (BEL Japan Inc). Their data were calculated using the method developed by Brunauer–Emmett–Teller.

Adsorption studies

The reactive yellow dye (RY160) (structure presented in Fig. 1a) was used as adsorptive in this study. 1.00 g RY160 was dissolved in deionized water to get a 1000 mg/L stock solution. Different working solutions were prepared by diluting the stock solution and their absorbance was measured by UV–visible spectrophotometer (Shimadzu UV- 2600) at wavelength 425 nm. The absorbance values were plotted against concentration to obtain a standard curve with correlation coefficient (R^2)= 0.99 (Fig. 1 b and c).

The batch adsorption experiments were carried out at room temperature (25°C) in 250 mL stopper conical flasks. A selected weight of the adsorbent was immersed in 100 mL of dye solution and shacked at 120 rpm using mechanical shaker (SK-L180 pro, China). The effect of contact time, adsorbent dosage, pH and dye concentration were studied to attain the optimum conditions. Samples were withdrawn at definite time intervals, filtered, and the remaining RY160 concentration in the filtrate was measured as described above.

All the experiments were carried out three times and the mean values of the results were calculated. The percent relative standard deviations were calculated and the values greater than 5% were rejected.
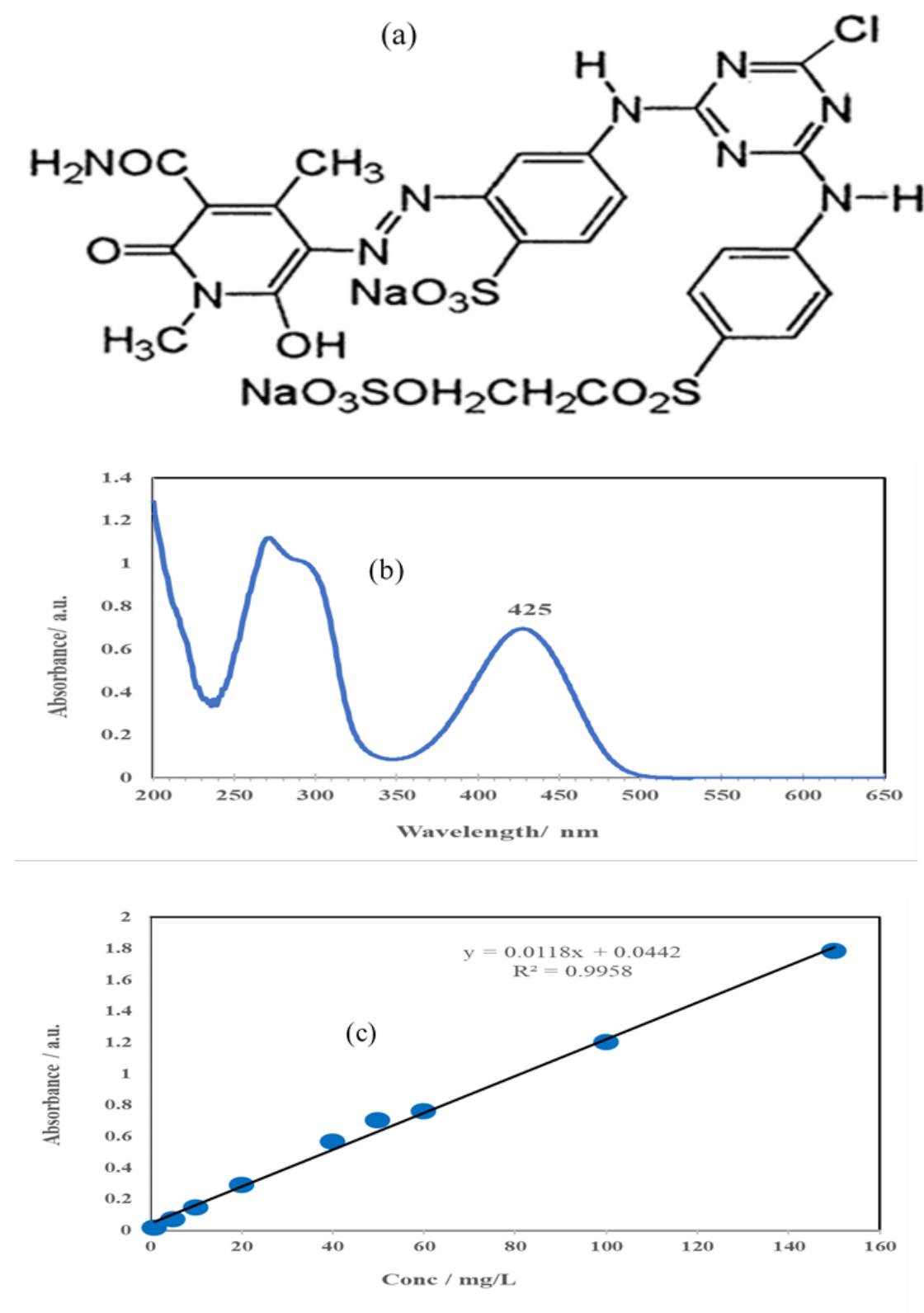
Fig. 1. (a) Structure of reactive yellow 160 dye used as adsorptive (b) UV-Visible spectrum of the RY160 dye. (c) standard curve for RY160 dye

Effect of adsorbent dosage

The adsorbent dosage was varied from 0.2 to 2.2 g/L using a volume of 100 mL of 50 mg/L of dye solution at the equilibration time for each adsorbent.

Effect of pH

To study the effect of acidic and alkaline medium on the adsorption process, different initial pH (2, 5, 7, 9 and 11) were prepared and used at the optimum time and dosage of the adsorption of RY 160 on the prepared samples.

Adsorption isotherms

Adsorption isotherm experiments were performed by shaking dye solutions of different initial concentrations (50–150 mg/L) using the optimum dosage of each adsorbent at the optimum time and pH. Freundlich, Langmuir and Dubinin–Radushkevich (D–R) isotherm are the three different adsorption isotherms that were used to describe the data of RY160 adsorption onto the prepared alumina nanoparticles [16].

Langmuir and Freundlich isotherms

Langmuir and Freundlich equations are the most widely implemented models to describe the relationship between equilibrium dye uptake (q_e) and final concentrations (C_e) at equilibrium [20]. Langmuir adsorption isotherm suggests a monolayer adsorption on the surface of adsorbent and the linear form of Langmuir isotherm model is given by the relationship:

$$C_e / C_{ads} = 1/Qb + C_e/Q \qquad (1)$$

where C_e (mg/L) is the concentration of dye in solution at equilibrium, C_{ads} is the amount of dye adsorbed per unit mass of the adsorbent. Q and b are the Langmuir constants related to the monolayer adsorption capacity and the adsorption energy, respectively.

Freundlich Isotherm

Freundlich isotherm is more general than Langmuir isotherm, hence it suggests a surface heterogeneity and the formation of multiple layers on the surface of the adsorbent.

The logarithmic form of Freundlich equation is given by:

$$\log q_e = \log K_f + \frac{1}{n} \log C_e \qquad (2)$$

where n and K_f are the Freundlich constants, which are related to the adsorption capacity of the adsorbent and the adsorption intensity or heterogeneity.

Dubinin-Radushkevich (D–R) isotherm

The D–R isotherm is more general than Langmuir isotherm because it does not assume a homogeneous surface or constant potential of adsorption [21]. The nature of adsorption process either chemical or physical can be predicted from the D–R model. The linear form of the D–R isotherm equation can be expressed as follows:

$$\ln q_e = \ln X_m - \beta \varepsilon^2 \qquad (3)$$

where q_e is the amount of dye adsorbed per unit mass of adsorbent (mol/g); X_m is the maximum adsorption capacity; β is the activity coefficient related to the mean adsorption energy; and ε is the Polanyi potential, which represented as:

$$\varepsilon = RT \ln(1 + 1/C_e) \qquad (4)$$

where R is the general gas constant (J/mol K), and T is the absolute temperature (K).

The adsorption energy can also be calculated using the following equation:

$$E = \frac{1}{\sqrt{-2\beta}} \qquad (5)$$

Results and Discussion

Characterization of prepared samples
   XRD analysis

The XRD patterns of Alo-600, Alo-800 and Alo-1050 (Alo-110 is completely amorphous aluminum hydroxide) are presented in Fig 2. The samples consist mainly of α-Al_2O_3 with different degree of crystallization according to JCPDS No.46-1212 [22,23]. The crystallite size of the samples was calculated from the Debye–Scherrer equation. The results indicate that the crystallite size of the samples Alo-600, Alo-800 and Alo-1050 are 4.47 nm, 5.34 nm and 45.97 nm, respectively. These values confirm the nano size of the prepared Al_2O_3 samples.

BET specific surface area

The nitrogen adsorption desorption data are presented in table 1. Their values indicate that, the BET specific surface area was 137.4, 118.3 and 59.8 m²/g for the samples Alo-600, Alo-800 and Alo-1050, respectively. It is noted that the BET surface area decreases with increasing heat treatment due to the increase in crystallite size as confirmed from XRD results [24]. The values of pore volume and pore size have no significant change for the samples.
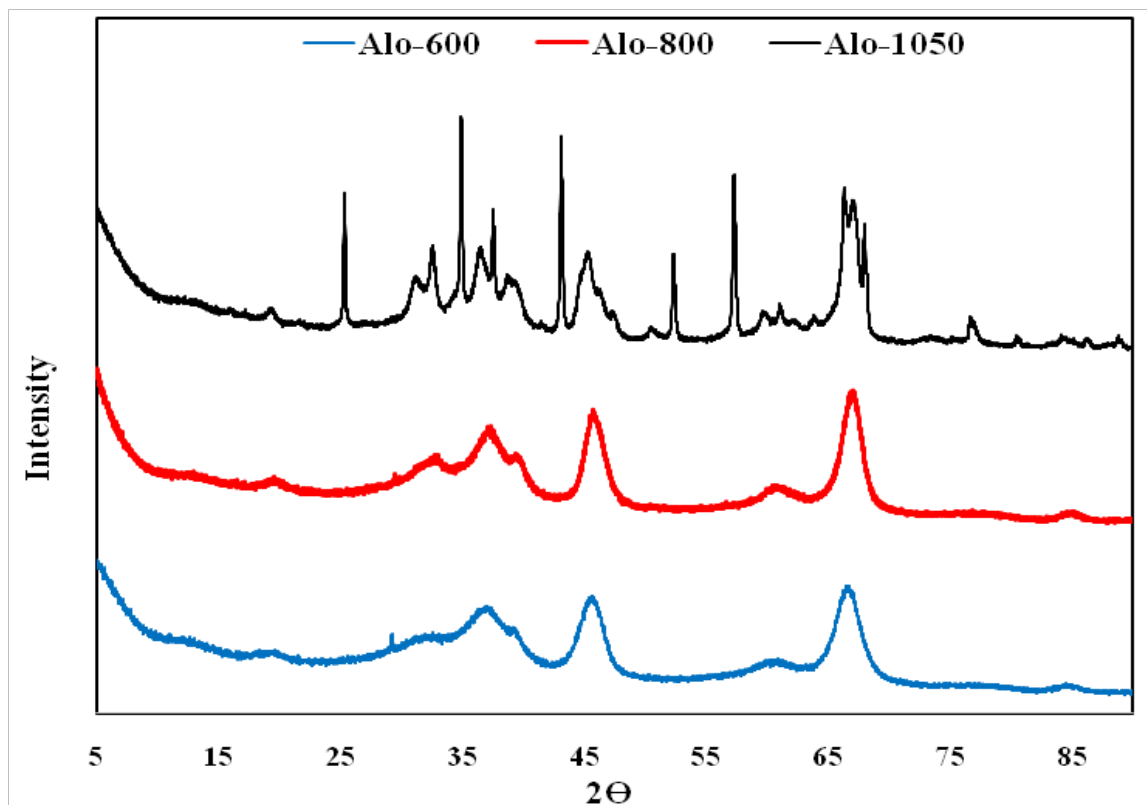
Fig. 2. XRD pattern of the alumina nanoparticles heated at different temperatures.

TABLE 1. Some characteristics of the prepared alumina.

Sample	Pore volume (cm³/g)	Pore diameter (nm)	S_{BET} (m²/g)
Alo-110	0.001	6.39	---
Alo-600	0.272	9.20	137.4
Alo-800	0.272	7.92	118.3
Alo-1050	0.215	14.40	59.8

SEM and EDAX

The general morphologies of the as-prepared Alo-110, and Alo-600, were analyzed by SEM in Fig. 4(a) and (b), respectively, which shows small particle size, uniform morphology and narrow size distribution of the synthesized particles. As shown in Fig. 3(a), the size of particles was also found to be in the nano-range which is in a good agreement with XRD data. The EDAX analysis of the sample Alo-600 (Fig. 3(c)) indicated that the sample is composed only from aluminum and oxygen confirming the formation of crystalline aluminum oxide.

FTIR

Figure 4 shows the FTIR spectra of the prepared samples before and after the adsorption of the dye. The band at 3445 cm⁻¹ is related to the stretching vibration of adsorbed water [25]. While the band at 1636 cm⁻¹ is attributed to the bending vibration of adsorbed water. The strong broad band between 1000 and 400 cm⁻¹ is assigned to the vibration of Al-O existed under 750 °C which clearly observed for sample Alo-600 [26]. There is no observable change for the FTIR before and after the adsorption process indicating that the adsorption may takes place physically on the surface of alumina nanoparticles samples in the current study.
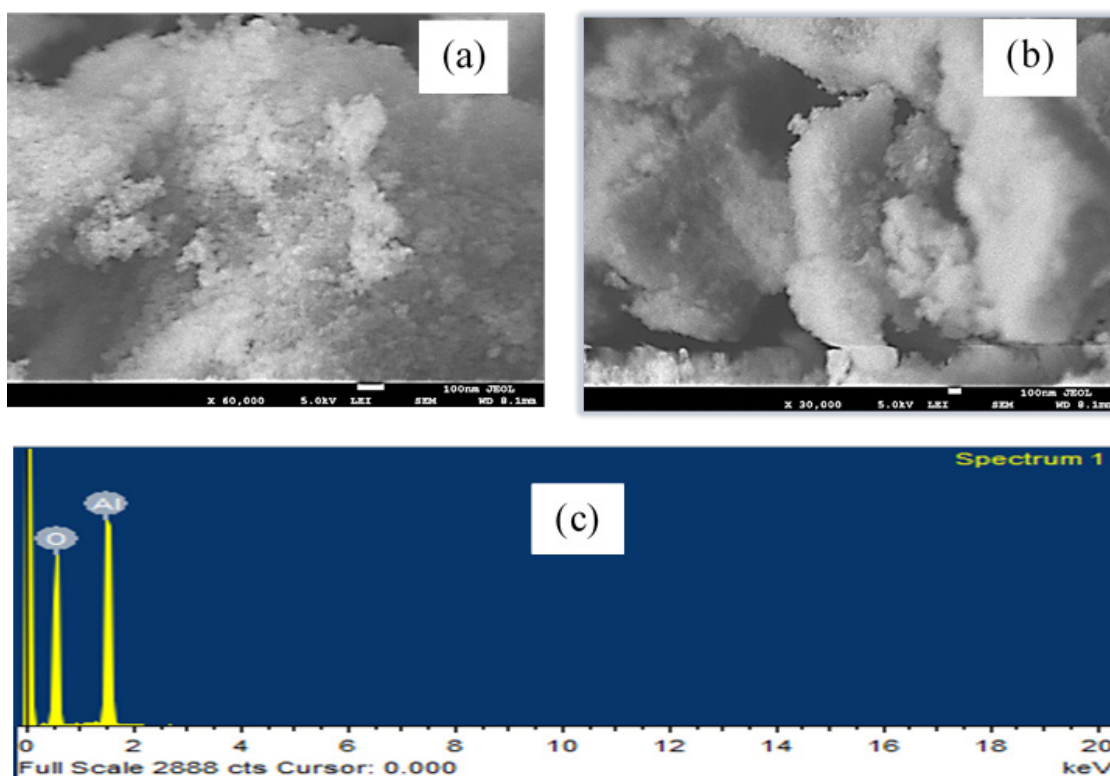
Fig. 3. SEM analysis of sample (a) Alo-110 and (b) Alo-600 and EDAX of sample (c)Alo-600.
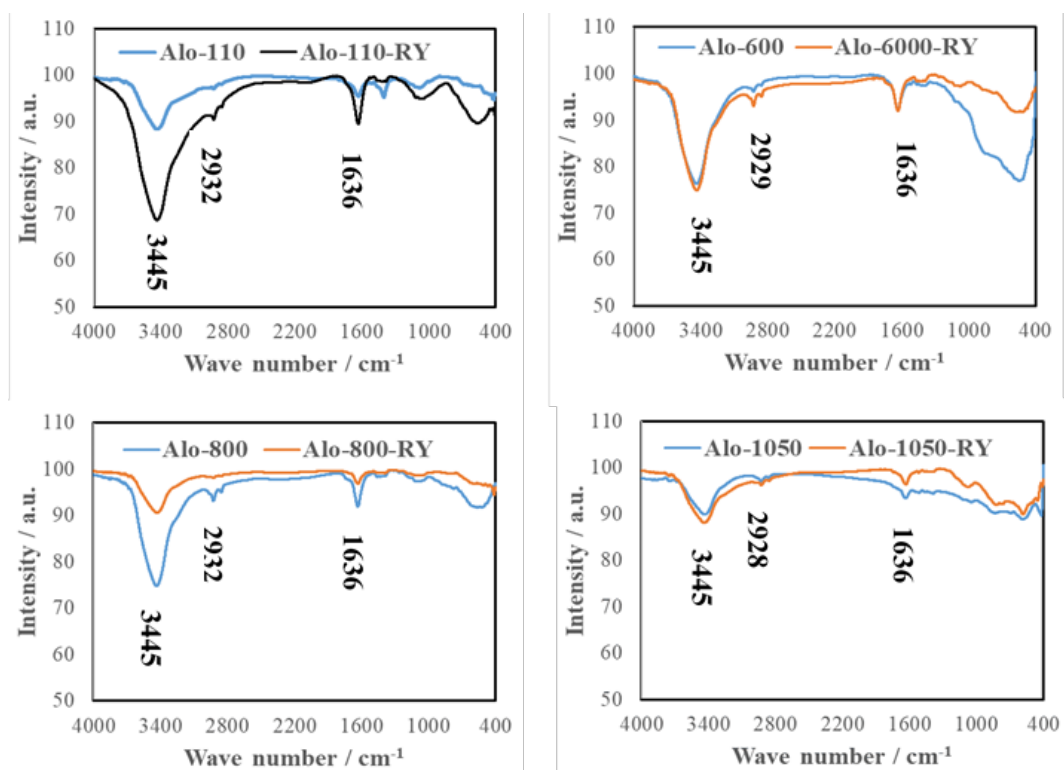

Fig. 4. FTIR analysis of the alumina nanoparticles before and after the adsorption of reactive yellow 160 dye.

Adsorption Studies

Effect of contact time

The effect of contact time on the removal of RY160 using the as prepared samples are presented in Fig. 5. The adsorption process takes place in two steps. The first step is the rapid one and takes place in the first five minutes. Then the rate of adsorption slows down gradually in the second step till the equilibrium takes place. The optimum contact time was found to be 10 min for Alo-110 and 80 min for the other samples, therefore, these optimum values will be implemented for the rest of experiments. As seen on Fig. 5, almost 100% of RY160 was removed by Alo-110 after 10 min of contact time, while the percentage removal achieved by other samples were 93.3%, 63.5% and 46.1% for the samples Alo-600, Alo-800 and Alo-1050, respectively. Also, it can be observed that, as the heat treatment of the adsorbent increase the percentage removal of the adsorptive decrease. This could be related to the sintering of the particles and the increase in the particle size with the increase of heat treatment, consequently the surface area decreased and the adsorptivity will be decrease as a result of the decrease of the available surface for adsorption [27].

Effect of dose

Fig. 6 presents the effect of adsorbent dosage on the removal of RY160 using the prepared samples of nano alumina. The results revealed that, the percentage removal of RY160 increased with increasing the dosage of the four adsorbents used till a certain optimum dose where the adsorption reach equilibrium and levelled off due to the formation of aggregates at higher dosages [10]. Alo-110 and Alo-600 were the most efficient adsorbents as could be observed in Fig. 6. They achieved 100% percentage removal of the dye at dosage 1 and 1.2 g/L respectively. On the other hand, the Alo-800 and Alo-1050 achieved 85% and 61% removal of the dye at dosage 1.6 and 2 g/L, respectively. Alo-110 exhibited the highest percentage removal of the reactive yellow 160 due to its nano sized particles and the presence of hydroxyl group (amorphous $Al(OH)_3$) as confirmed by XRD.

Effect of pH

The pH has an essential role in the adsorption process due to the difference of the charges existed on the surface of adsorbent in different pH medium which may increase or decrease the efficiency of the adsorption process. The effect of pH variation on the adsorption of RY160 onto the surface of nano alumina samples is presented in Fig. 7. Two trends can be observed, the first trend exhibited by sample Alo-110 which composed of amorphous nano

$Al(OH)_3$. Alo-110 exhibited the highest adsorption of RY160 at pH 5, and the adsorption decreased with increasing pH. This trend can be explained as follow: at acidic medium the function groups of the dye are negatively charged and the hydroxyl groups of the adsorbent are protonated (positively charged) leading to attraction and increase in the adsorption process. While in basic medium a repulsion takes place between the negatively charged function groups of the dye and the hydroxyl groups of the adsorbent. Therefore, the sample Alo-110 showed its highest ability to adsorb the dye at pH 5. The second trend exhibited by the three samples Alo-600, Alo-800 and Alo-1050 which consists only of α-Al_2O_3 crystalline phase. They showed high adsorption of the dye at strong acid medium due to the strong attraction of dye functional groups and the surface of alumina. Meanwhile the adsorption decreased with increasing pH in basic medium due to the repulsion and competition between the negatively charged functional group of the dye and the hydroxyl group of the basic medium. These results agree with the previous data in literature [28].

Isotherm models

Langmuir isotherm

Langmuir isotherm model suggested that, the adsorption takes place uniformly on the adsorbent active sites, and once the adsorbate occupies certain site, no further adsorption can take place on this site [20]. The parameters of Langmuir isotherm can be used to indicate the affinity between the adsorbent and adsorbate.

The adsorption of RY160 onto the nano alumina samples (Alo-110, Alo-600, Alo-800 and Alo-1050) was best fitted to Langmuir isotherm with correlation coefficient values (R^2) = 0.9924, 0.9982, 0.9995 and 0.9685, for the above-mentioned samples, respectively (Table 2, Fig. 8a). This reveal that the surface of nano alumina was covered by a monolayer of the dye RY160. The monolayer adsorption capacity Q_{max} in table 2 indicated the following sequence for adsorption of RY160: Alo-600 > Alo-800 > Alo-1050 > Alo-110.

The results of the first three samples Alo-600, Alo-800 and Alo-1050 (nano Al_2O_3) are in agreement with the obtained data in Figs. 5, 6 and 7. On the other hand Alo-110 (amorphous $Al(OH)_3$) which exhibited the highest % removal in Fig. 5,6 and 7 showed the lowest monolayer adsorption capacity (table 2). This may indicate that the adsorption of RY160 on the surface of Alo-110 is controlled by other mechanism rather than the monolayer suggested by Langmuir.
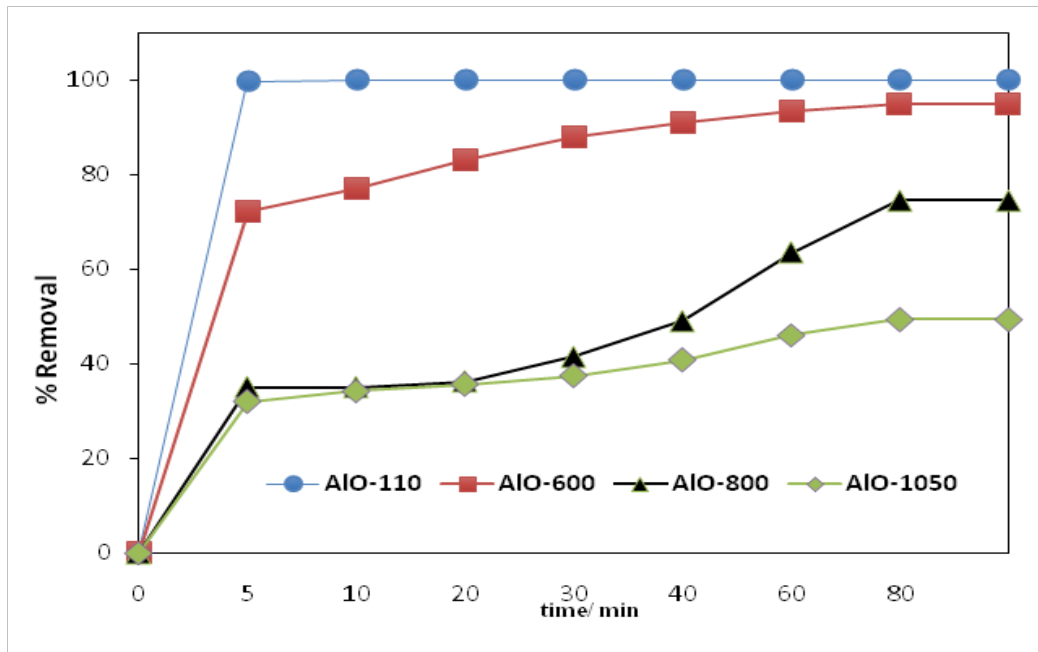
Fig. 5. Effect of contact time for the removal of RY160 onto alumina nanoparticles (RY160 conc. 50 mg/L, dosage 1 g/L pH 5).
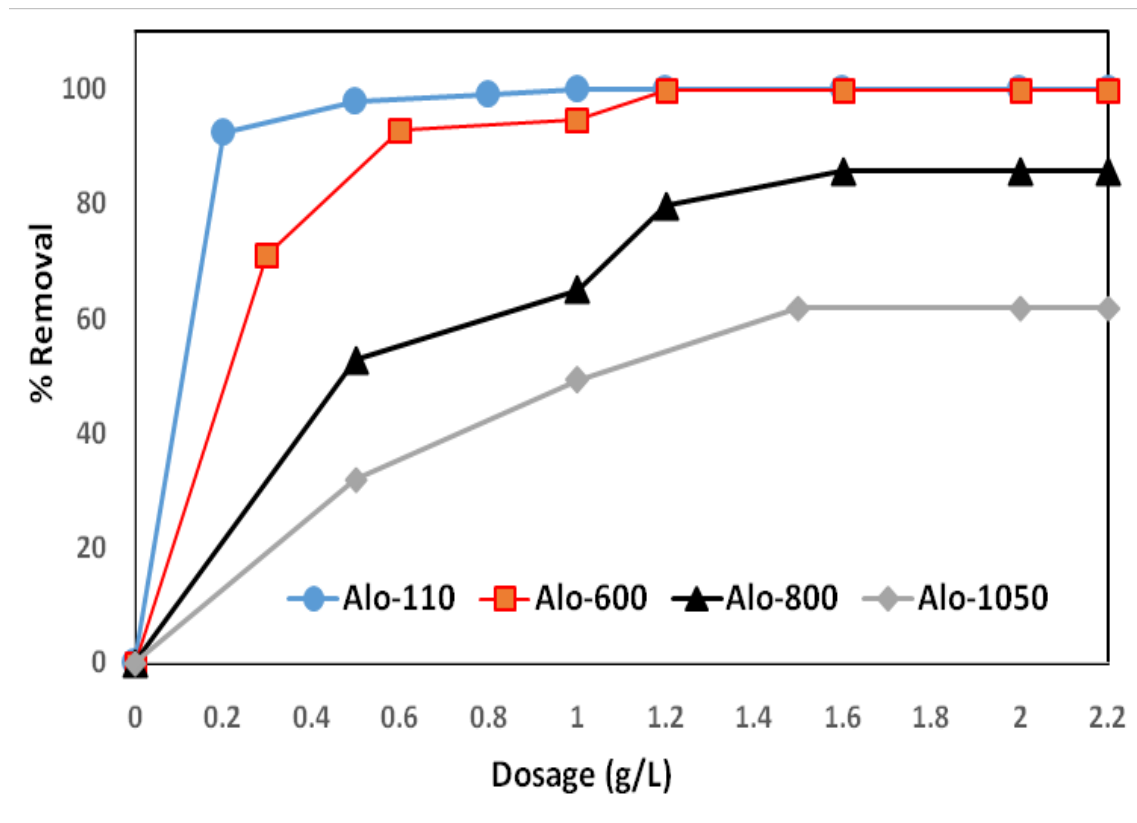

Fig. 6. Effect of dosage on the removal of RY160 onto alumina nanoparticles (RY160 conc. 50 mg/L, contact time; Alo-110 10 min, Alo-600, Alo-800 and Alo-1050 80 min, pH 5).
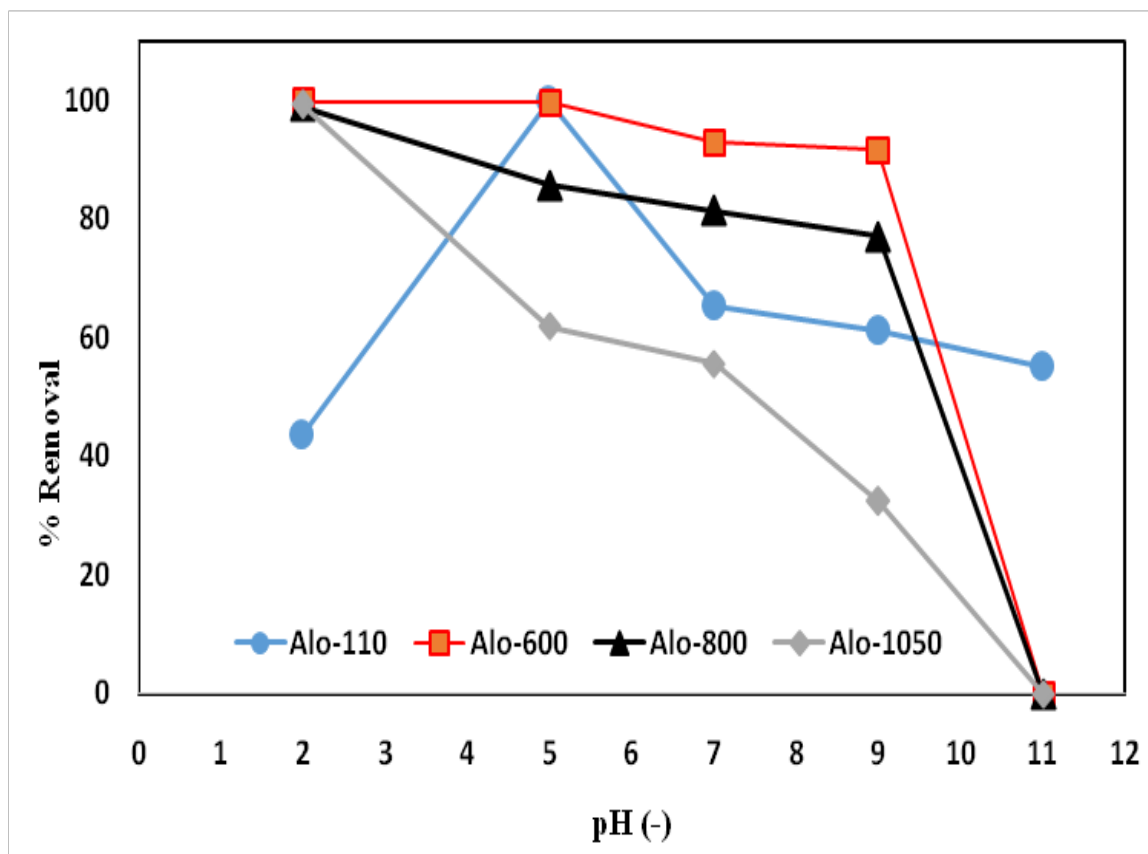
Fig. 7. Effect of pH on the adsorption of RY160 onto alumina nanoparticles. (RY160 conc. 50 mg/L, contact time; Alo-110 10 min, Alo-600, Alo-800 and Alo-1050 80 min).

Freundlich isotherm.

Freundlich isotherm is more general than Langmuir isotherm, because it deals with surface heterogeneity and does not assume monolayer adsorption. The Freundlich parameters K_f and 1/n are used to explain the affinity between the adsorbent and adsorbate [29]. A low value of 1/n is an indicator for high affinity between adsorbent and adsorbate, and a high K_f value point out that the adsorbent has a high uptake capacity. The R^2 in Table 2 and Fig. 8b for the samples Alo-110, Alo- 600, Alo-800, and Alo-1050 were 0.987, 0.914, 0.915 and 0.521 respectively. These values indicated that only the adsorption of RY 160 on the surface of Alo-110 can be described by Freundlich isotherm model. The high value of K_f for sample Alo-110 in table 2 indicates the high affinity of this sample for the adsorption of RY160 from aqueous solutions. This behavior of Alo-110 indicate that the adsorption of RY160 onto Alo-110 can be described by both models Langmuir and Freundlich. Thus, explain the lower Langmuir adsorption capacity than could be expected.

D–R isotherm.

Langmuir and Freundlich isotherms did not give information about the adsorption mechanism. The nature of the adsorption process as chemical or physical can be predicted from the D–R isotherm model. The D-R plots of the adsorption of RY160 onto the different alumina samples are presented in Fig. 8c. The model parameters are also presented in Table 2. The mean free energy of adsorption calculated from the D-R plot can indicate the type of adsorption chemical or physical. The positive values of the energy of adsorption E in Table 2 pointed out that the adsorption of RY160 on the surface of nano alumina samples is endothermic process [30]. The values of mean adsorption energy in Table 2 were 17.05, 29.54, 25.28 and 33.37 kJ/ mol for the nano alumina samples Alo-110, Alo-600, Alo-800 and Alo-1050, respectively. These values of adsorption free energy <40 kJ/mol) indicated that, the adsorption process takes place physically [31,32].
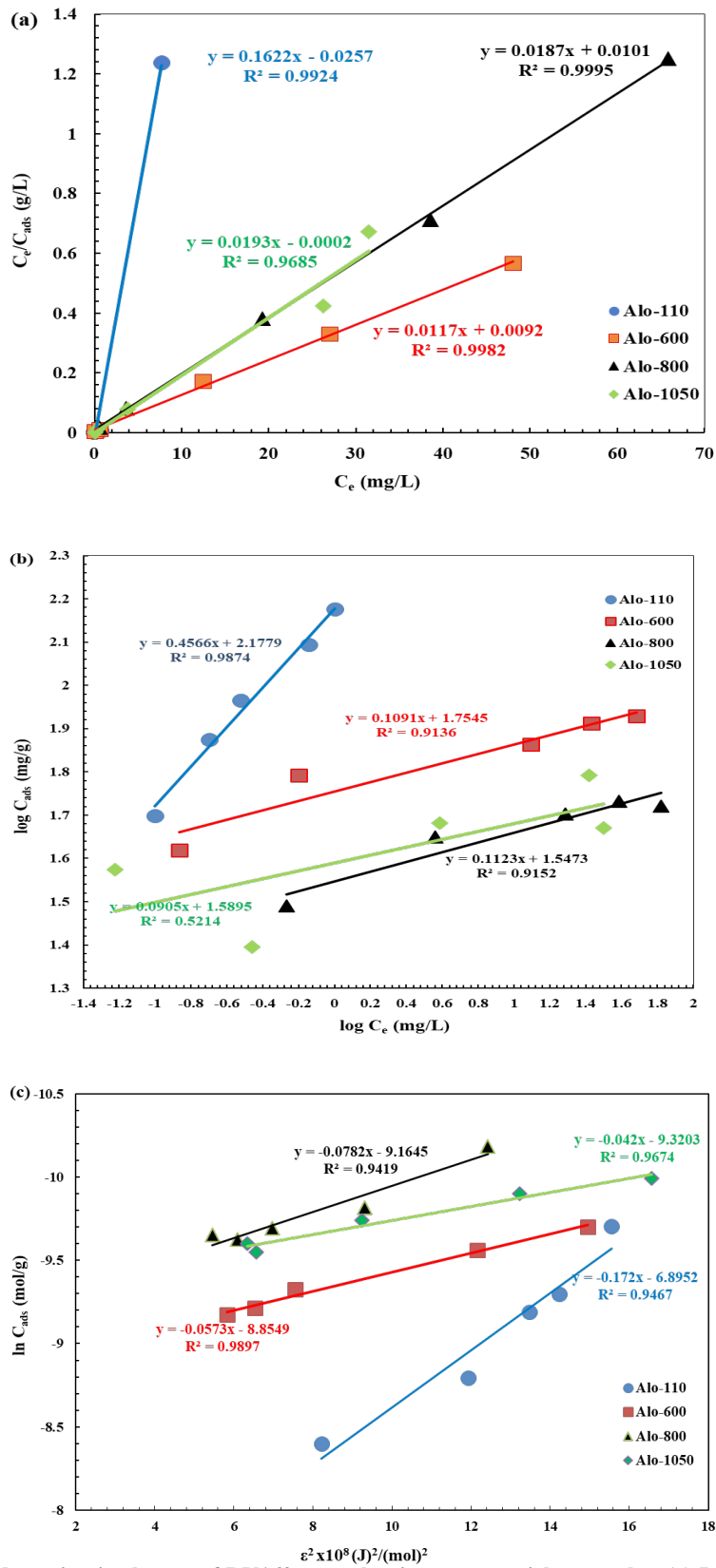
Fig. 8. Adsorption isotherms of RY160 onto alumina nanoparticles samples. (a) Langmuir, (b) Freundlich and (c) D-R models.

TABLE 2. Summary of isotherm model parameters.

Sample	Freundlich model			Langmuir model			D-R model		
	K_f	$1/n$	R^2	Q_{max}(mg/g)	$1/b$	R^2	X_m(mol/g)	b(mol²/j²)	E (KJ/mol)
Alo-110	150.62	0.46	0.987	6.16	0.16	0.992	1.0726×10^{-3}	-0.172×10^{-8}	17.05
Alo-600	56.82	0.11	0.914	85.47	0.79	0.998	1.4268×10^{-4}	-0.057×10^{-8}	29.54
Alo-800	35.26	0.11	0.915	53.48	0.54	0.999	1.047×10^{-4}	-0.078×10^{-8}	25.28
Alo-1050	38.86	0.10	0.521	51.81	0.01	0.968	9.349×10^{-5}	-0.049×10^{-8}	33.37

Conclusion

The alumina nanoparticles prepared from waste alumnium metal has considerable potential for the removal of reactive yellow 160 dye from aqueous solution under different conditions and over a wide range of concentrations. The results showed that the three heated samples are consisted mainly of Al_2O_3 crystalline phase in the nano scale. The adsorbability of the prepared samples were in the order Alo-110> Alo-600 > Alo-800 > Alo-1050 with percentage removal reached 100% for Alo-110. The adsorption data were best described by Langmuir isotherm model for the prepared samples indicating a monolayer surface adsorption. The adsorption process was confirmed to be endothermic and the adsorption takes place physically.

Conflicts of interest

The authors declare that they have no conflict of interest.

References

1. Singh H., Chauhan G. , Jain A.K. , Sharma, S. Adsorptive potential of agricultural wastes for removal of dyes from aqueous solutions, *Journal of Environmental Chemical Engineering,* **5,** 122-135 (2017).

2. Li, Z., Li, L., Hu, D., Gao, C., Xiong, J., Jiang, H., Li, W. Efficient removal of heavy metal ions and organic dyes with cucurbit [8] uril-functionalized chitosan. *Journal of Colloid and Interface Science.* **539**, 400-413 (2019).

3. Pérez-Morales, J. M., Sánchez-Galván, G., Olguín, E. J. Continuous dye adsorption and desorption on an invasive macrophyte (*Salvinia minima*). *Environmental Science and Pollution Research*. 1-16 (2019).

4. R, J., J, J. Simultaneous removal of binary dye from textile effluent using cobalt ferrite-alginate nanocomposite: Performance and mechanism. *Microchemical Journal*. **145**, 791-800 (2019).

5. Gharbani, P. Modeling and optimization of reactive yellow 145 dye removal process onto synthesized MnO_X-CeO_2 using response surface methodology. *Colloids and Surfaces A: Physicochemical and Engineering Aspects*. **548**, 191-197 (2018).

6. Wong, S., Tumari, H. H., Ngadi, N., Mohamed, N. B., Hassan, O., Mat, R., Saidina Amin, N. A. Adsorption of anionic dyes on spent tea leaves modified with polyethyleneimine (PEI-STL). *Journal of Cleaner Production*. **206**, 394-406 (2019).

7. Radwan, E. K., El-Wakeel, S. T., Gad-Allah, T. A. Effects of activation conditions on the structural and adsorption characteristics of pinecones derived activated carbons. J. Dispersion Sci. Tech. (2018). (10.1080/01932691.2018.1467327)

8. Embaby, M. A., Ghafar, H. H. A., Shakdofa, M. M. E., Khalil, N. M., Radwan, E. K. Removal of iron and manganese from aqueous solution using some clay minerals collected from Saudi Arabia. *Desalination and Water Treatment*. **65**, 259-266 (2017). (10.5004/dwt.2017.20270)

9. El-Wakeel, S. T., Radwan, E. K., Abdel Ghafar, H. H., Moursy, A. S. Humic acid-carbon hybrid material as lead(II) ions adsorbent. *Desalination and Water Treatment*. **74**, 216-223 (2017). (10.5004/dwt.2017.20584)

10. Abdel Ghafar, H. H., Embaby, M. A., Radwan, E. K., Abdel-Aty, A. M. Biosorptive removal of basic dye methylene blue using raw and $CaCl_2$ treated biomass of green microalga *Scenedesmus obliquus*. *Desalination and Water Treatment*. **81**, 274-281 (2017). (10.5004/dwt.2017.21108)

11.   Radwan, E. K., Ghafar, H. H. A., Moursy, A. S., Langford, C. H., Bedair, A. H., Achari, G. Preparation and characterization of humic acid–carbon hybrid materials as adsorbents for organic micro-pollutants. *Environmental Science and Pollution Research*. **22**, 12035-12049 (2015). (10.1007/s11356-015-4468-9)

12.   Abdel Ghafar, H. H., Salem, T., Radwan, E. K., Atef El-Sayed, A., Embaby, M. A., Salama, M. Modification of waste wool fiber as low cost adsorbent for the removal of methylene blue from aqueous solution. *Egyptian Journal of Chemistry*. **60**, 395-406 (2017). (10.21608/ejchem.2017.687.1023)

13.   El-Wakeel, S. T., Radwan, E. K., El-Kalliny, A. S., Gad-Allah, T. A., El-Sherif, I. Y. Structural, magnetic and adsorption characteristics of magnetite nanoparticles prepared from spent pickle liquor. *International journal of chemtech research*. **9**, 373-382 (2016).

14.   Metwally, B. S., El-Sayed, A. A., Radwan, E. K., Hamouda, A. S., El-Sheikh, M. N., Salama, M. Fabrication, characterization, and dye adsorption capability of recycled modified polyamide nanofibers. *Egyptian Journal of Chemistry*. **61**, 867-882 (2018). (10.21608/ejchem.2018.3967.1367)

15.   H. H. Abdel Ghafar, M. Salama, E.K. Radwan, T. Salem, Recycling of pre-consumer viscose waste fibers for the removal of cationic dye from aqueous solution. Egypt. J. Chem. Vol. 62, No.6, pp.1455 – 1465 (2019).

16.   Imran Ali, Omar M.L. Alharbi, Zeid A. Alothman, Ahmad Yacine Badjah, Abdulrahman Alwarthan, Al Arsh Basheer. Artificial neural network modelling of amido black dye sorption on iron composite nano material: Kinetics and thermodynamics studies. Journal of Molecular Liquids 250 1–8(2018)

17.   N.F. El Boraei, M.A.M. Ibrahim. Black binary nickel cobalt oxide nano-powder prepared by cathodic electrodeposition; characterization and its efficient application on removing the Remazol Red textile dye from aqueous solution. Materials Chemistry and Physics 238, 121894(2019)

18.   Vasanthakumar Arumugam, Pavithra Sriram, Ta-Jen Yen, Gyanasivan Govindsamy Redhi, Robert Moonsamy Gengan . Nano-material as an excellent catalyst for reducing a series of nitroanilines and dyes: triphosphonated ionic liquid- CuFe2O4-

19.   Md. Aminul Islam, Imran Ali, S.M. Abdul Karim, Md. Shakhawat Hossain Firoz, Al-Nakib Chowdhury, David W. Morton, Michael J. Angove. Removal of dye from polluted water using novel nano manganese oxidebased Materials. Journal of Water Process Engineering 32, 100911(2019)

20.   Langmuir, The adsorption of gases on plane surfaces of glass, mica and platinum, J. Am. Chem. Soc., 40, 1361–1403(1918) .

21.   M.M. Dubinin, E. Zaverina, L. Radushkevich, Sorption and structure of active carbons. I. Adsorption of organic vapors, Zhurnal Fizicheskoi Khimii, 21, 1351–1362(1947).

22.   Yu YOU, Akihiko ITO, Rong TU and Takashi GOTO, Orientation control of ¡-Al$_2$O$_3$ films prepared by laser chemical vapor deposition using a diode laser. Journal of the Ceramic Society of Japan 118 [5] 366-369 (2010)

23.   B. D. Cullity, Elements of X-Ray Diffraction? Addison- Wesly Publishing, Notre Dame, Indiana, 3rd edition, (1976).

24.   S. Cava, S.M. Tebcherani, I.A. Souza, S.A. Pianaro, C.A. Paskocimas, E. Longo, J.A. Varela. Structural characterization of phase transition of Al$_2$O$_3$ nanopowders obtained by polymeric precursor method. Materials Chemistry and Physics 103, 394–399 (2007).

25.   Ivanić, M.; Vdović, N.; Barreto, S. d.; Bermanec, V.; Sondi, I., Mineralogy, surface properties and electrokinetic behaviour of kaolin clays from the naturally occurring pegmatite deposits. Geologia Croatica**, 68 (2), 139-145 (2015).

26.   Seyed Ali Hosseini, Aligholi Niaei, Dariush Salari, Production of γ-Al$_2$O$_3$ from Kaolin, Open J. Phys. Chem., 1, 23-27 (2011).

27.   Hany H. Abdel Ghafar, Gomaa A.M. Ali, Osama A. Fouad, Salah A. Makhlouf. Enhancement of adsorption efficiency of methylene blue on Co3O4/SiO2 Nanocomposite. Desalination and water treatment. 53 2980–2989(2015)

28.   Toutounchi, S.; Shariati, S.; Mahanpoor, K., Synthesis of nano-sized magnetite mesoporous carbon for removal of Reactive Yellow dye from aqueous solutions. *Applied Organometallic Chemistry* **2019,***33* (9), e5046.

REMOVAL OF REACTIVE YELLOW 160 FROM AQUEOUS SOLUTION BY ALUMINA ...

2899

29. M.B. Desta, Batch sorption experiments: Langmuir and Freundlich isotherm studies for the adsorption of textile metal ions onto Teff Straw (*Eragrostis tef*) agricultural waste, J. Thermodyn., 2013 1–6(2013).

30. F.G. Helfferich, Ion Exchange, Courier Corporation, (1962).

31. W. Rieman, H.F. Walton, Ion Exchange in Analytical Chemistry: International Series of Monographs in Analytical Chemistry, Elsevier, (2013).

32. H.S. Ibrahim, N.S. Ammar, H.H. Abdel Ghafar, M. Farahat, Adsorption of Cd(II), Cu(II) and Pb(II) using recycled waste glass: equilibrium and kinetic studies, Desal. Wat. Treat., 48, 320–328(2012).